LUND UNIVERSITY
DIVISION OF PHYSICAL CHEMISTRY

Probing the Intermolecular Interactions of Lactoferrin

Maxim Morin

Bachelor of Science Thesis
Lund June 2013

LUND UNIVERSITY

Table of Contents

Abstract

In this work the effect of pH and ionic strength on interactions for the globular protein lactoferrin has been studied using static and dynamic light scattering. The interactions were investigated in terms of the second virial coefficient, $B_{2,}$ and the collective diffusion coefficient, D_{coll}, at different concentrations of electrolyte. The conditions investigated in this work will serve as a stable point-of-departure from which we will set out, in a controlled way, to explore the phase diagram with the aim to use lactoferrin as a model protein to investigate the role of patchy attractive interactions, i.e. charged groups and hydrophobic groups are unevenly distributed at the protein surface. The charged groups depend strongly on both pH and ionic strength. The overall reproducibility and stability against time are crucial and shown here to be highly satisfactory. From determination of B_2 the interactions are found to be, at the investigated pH and ionic strength, overall repulsive and in agreement with computer simulations and preliminary SAXS measurements. However, the collective diffusion coefficient appears to be, under the same conditions, not as repulsive which calls for further measurements and analysis.

Introduction

Protein interactions have two main contributions, the first comes from electrostatics and the second one comes from hydrophobic interactions. The interplay of these two gives the true picture of protein interactions [20]. Interactions between proteins are very complex which is partly due to properties of the constituent amino acids. Some of them are either basic or acidic, some of them contain polar groups which may be partly dissociated while other amino acids have hydrophobic groups. This means that the net charge of the proteins can be tuned by changing the pH of the solution [20]. By changing the charge, the strength and geometry of the electrostatic interactions are going to change, affecting the interactions between protein molecules, especially at low electrolyte concentrations where Coulomb interactions dominate. When the salt concentration increases, the electrostatic interactions become weaker due to screening and the effect of pH on protein interactions becomes more subtle [21]. The number of charged groups presented in proteins is large and there is no even distribution of these charges, instead they create patches which give a complex interface of the proteins. Besides that, tertiary and quaternary structures of proteins strongly depend on the hydrophobic effects arising from simultaneous presence of hydrophilic and hydrophobic groups [20]. Interactions between protein molecules also depend on these hydrophobic effects.

In addition, a salt-specific dependence was also shown for protein interactions where different monovalent salts followed the Hofmeister series which is strongly related to hydrofobicity [22]. At pH lower than the protein's isoelectric point (pH<pI), anions act as counterions and the double layer repulsion increases in the order NaSCN<NaI<NaCl following a reverse Hofmeister sequence while at pH higher than pI the counterions are cations and the double layer repulsions increases now for the direct Hofmeister sequence NaCl<NaI<NaSCN [22]. This was shown by light scattering measurements on lysozyme [12]. For the electrostatic forces, it was found that they dominate at lower electrolyte concentrations, but when the electrolyte concentration becomes significantly higher, the electrostatic forces become much weaker due to the screening effect. At high salt concentrations it is believed that non-electrostatic ion-specific forces, where dispersion forces play a dominant role, overcome the electrostatic forces [22]. Studies made on β-lactoglobulin (BLG) type A have shown that B_2 has a well pronounced minimum at ionic strength (controlled by KBr) around 0.25 M. But when the ionic strength was increased B_2 became positive again [20]. Same result was shown for appoferritin, where B_2 was first decreasing to approximately 150 mM (NaCl was used as

electrolyte), but when ionic strength was further increased B_2 values become positive again. We can make a conclusion from these two examples that the DLVO theory works at low ionic strengths, but fails at high ionic strengths. This is a direct evidence of non-monotonic intermolecular interactions [20].

We have chosen to study lactoferrin (LF) which is a water-soluble globular, iron-binding glycoprotein found in milk and colostrum at a concentration around 10 mg/mL. This is the second most abundant protein in milk after caseins. LF can also be found in tears, saliva, nasal and bronchial secretion, and urine [2]. The protein consists of 703 amino acids and has a molecular weight of 77-80 kDa [1, 2]. It is composed of a single polypeptide chain, which folds into two globular lobes (C- and N-terminal regions) connected by a α-helix as shown in Figure 1, providing flexibility to the molecule [2]. Both lobes include two domains which creates iron binding sites on each lobe. As shown in Figure 1, iron ions are located deep within the interdomain clefts. Blue cylinders represent α-helixes and violet arrows represent β-strands. On the C-Lobe one can also see carbohydrate moieties shown in ball and stick model.

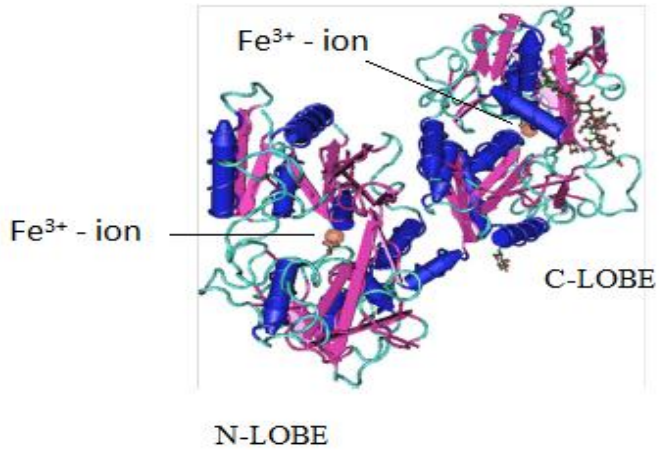

Figure 1. Three-dimensional structure of holo-lactoferrin at 2.8 Å resolution [2].

There are three different variants of LF depending on the iron ion saturation [1]. Iron-free LF is called apo LF, with one iron ion bound it is called monoferric LF, and the fully saturated with two iron ions bound is termed holo LF [1]. There is a small structural difference between the apoform and the holoform, where the free iron form has a more open conformation, compared to the iron saturated holo LF [2]. Under physiological conditions LF is positively charged with an isoelectric point located at a pH between 8.0 – 8.5 [2-4, 6].

LF has a strong iron-binding affinity and is the only protein from the transferrin family having the ability to retain iron over a wide range of pH [2], which is especially important at inflammatory sites where pH can decrease below 4.5 due to metabolic activity of bacteria [1]. LF plays an important role in several immunological functions. For example, LF controls the growth of bacteria by decreasing the level of free iron, Fe^{3+}, which is an essential factor in bacterial growth such as the iron-dependent bacteria *E. Coli* [1]. Also, by blocking viral receptors of cell membrane LF prevents viruses from entering and infecting cells [1]. LF can act as anti-inflammatory factor by reducing the production of pro-inflammatory cytokines (TNFα) [1]. It has also been found to be effective against cancer development.

Aggregation of proteins is important to study both from gaining a better biophysical understanding but also since there is a group of diseases termed Amyloidoses, where proteins aggregate and form insoluble clusters accumulating in different organs causing about 20 different pathological conditions [20]. By better understanding factors affecting interactions between proteins we can find ways how to cure disease caused by protein aggregation (such as Alzheimer's, Parkinson's etc.).

Regarding the solution behaviour of LF, previous work shows the formation of aggregates when the ionic strength is increased presumably due to simple screening of the salt [3]. However, a more intricate interplay has been found from computer simulations revealing that there are a stereo-specific attraction at certain orientations between two LF molecules. The strength of the attraction stems from a delicate balance between electrostatic and van der Waals forces. From the simulations it is found that when pH approaches the isoelectric point LF begin to form dimers at low ionic strength. The reason for this being a highly complementary physical bound between two proteins both, with a charged, attractive patch located at the surface [3]. The effect of having such patchy, anisotropic interactions is believed to alter the phase diagram rather drastically as compared to colloidal particles interacting via an isotropic, centro-symmetric interaction potential [24]. We are proposing to use LF as a model protein system to study the implications of patchy interactions, on the solution behaviour and phase diagram of LF.

In what follows, in the experimental section I will describe the techniques used for determination of concentrations, which is crucial for a quantitative analysis of the static light scattering. In the results and discussion I will present sample preparation protocols and measurements of the interactions between lactoferrin molecules and how they are affected to

some extent by small changes in pH, ionic strength and temperature. In the measurements of the second virial coefficient, B_2, from static light scattering, also the molecular weight is obtained. In parallel, collective diffusion coefficients obtained from dynamic light scattering are determined which also contain information regarding particle interactions. Results from preliminary SAXS measurements will also be shown. I conclude with a summary of conclusions and a future outlook.

Experimental section

UV-VIS Spectroscopy

The concentration of a protein in solution is determined by UV-vis spectroscopy by measurements of the absorbance as a function of wavelength. When light with initial intensity I_0 passes through a cuvette with length, L, containing molecules J, part of the light is absorbed by the sample giving a final intensity, I, which is lower than the initial intensity, due to absorption. The fraction between the final and the initial intensities of light is called the transmittance, denoted T,

$$T = \frac{I}{I_0} \qquad \text{Eq. 1}$$

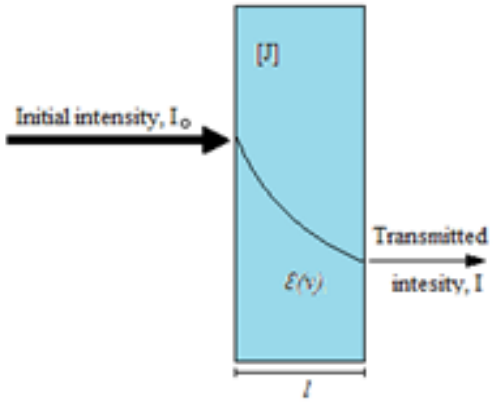

Figure 2. Schematic description of how the intensity of light, traveling through the sample, decreases exponentially with the length of the sample. *[J]* is the concentration, $\boldsymbol{\varepsilon(\nu)}$ is the molar absorption coefficient and *l* is the length of the sample.

There is a logarithmic dependence between T and the absorption coefficient or extinction coefficient, ε which is characteristic to the molecules in the sample, the total concentration [J] and the path length of the cuvette l,

$$T = \frac{I}{I_0} = 10^{-\varepsilon[J]l} \qquad \text{Eq. 2}$$

The transmittance and the absorbance, *A*, are simply related by

$$A = -logT = log\frac{I_0}{I} \qquad \text{Eq. 3}$$

By introducing equation 2 into the expression for the absorbance the Beer-Lambert law is obtained

$$A = \varepsilon cl \qquad \text{Eq. 4}$$

In order to determine ε a series of measurements must be performed of known concentrations. The obtained absorbance maxima (A_{max}) of each concentration should then be plotted as a function of concentration (proteins display a characteristic absorption peak at 280 nm, which comes from the amino acids tryptophan, tyrosine and cysteine [10]). A straight line is obtained and from the slope the extinction coefficient is determined.

Static Light Scattering

In Static light scattering the time-averaged mean intensity of the scattered electrical field is measured as a function of angle. From the scattered intensity important molecular information can be obtained such as the molecular weight, M_w, and second virial coefficient, B_2, by measuring as a function of concentration and applying the so-called Zimm equation [5]

$$\frac{K \cdot c}{R_\theta} = \frac{1}{M_w} + \frac{2 \cdot N_A \cdot B_2}{M_w^2} \cdot c \qquad \text{Eq. 5}$$

here, *K* is an optical constant with units [mol·m^{-2}·kg^{-2}], *c* is the concentration in [kg/m^3], R_θ is the Rayleigh ratio at angle θ and N_A is Avogadro's constant ($6.022 \cdot 10^{23}$ mol^{-1}). The optical constant is defined as

$$K = \frac{4\pi n_0^2 \left(\frac{dn}{dc}\right)^2}{N_A \lambda^4} \qquad \text{Eq. 6}$$

n_0 is the refractive index of the solvent, (d*n*/d*c*) is the refractive index increment and λ is the wavelength of light. The second virial coefficient, B_2, is defined as

$$B_2 = 2\pi \int_0^{\infty} r^2 (1 - e^{-U(r)\beta}) dr \qquad \text{Eq. 7}$$

where *U(r)* is the important interaction potential and β is $1/k_BT$. B_2 has a unit of volume [m^3] and contains important information about molecular interactions. The Zimm equation can be used in a simplified type of Zimm plot by measuring the scattered intensity at angles corresponding to values much smaller than the size of the protein, where there is no angular dependence. By plotting Kc/R_θ as a function of concentration the molecular weight is obtained from the intercept, and the second virial coefficient from the slope

$$B_2 = \frac{Slope \cdot M_w^2}{2 \cdot N_A} \qquad \text{Eq. 8}$$

Is is useful to normalize the second virial coefficient against the corresponding hard sphere value

$$B_2^* = \frac{B_2}{B_2^{HS}} \qquad \text{Eq. 9}$$

Where the interaction potential for hard spheres is infinitely repulsive at distances smaller than the hard sphere diameter, σ, and zero everywhere else

$$U(r) = \begin{cases} \infty, & r \leq \sigma \\ 0, & r > \sigma \end{cases} \quad (\sigma \text{ is the hard sphere diameter})$$

The expression for the second virial coefficient of hard spheres is

$$\begin{aligned} B_2^{HS} &= 2\pi \int_0^{\sigma} r^2 \left(1 - e^{(-U(r)=\infty)\beta}\right) dr + 2\pi \int_{\sigma}^{\infty} r^2 \left(1 - e^{(-U(r)=0)\beta}\right) dr \\ &= 2\pi \int_0^{\sigma} r^2 dr + 0 = \\ &= 2\pi \frac{\sigma^3}{3} \end{aligned} \qquad \text{Eq. 10}$$

In the expression for the normalized B_2^* there is a cubic dependence of the inverse hard sphere diameter or radius used in the normalization. This makes it highly sensitive to which size is used as the hard sphere radius.

$$B_2^* = \frac{3B_2}{2\pi\sigma^3} \qquad \text{Eq. 11}$$

Dynamic Light Scattering

In Dynamic light scattering the dynamic properties of colloidal particles are measured by the time-dependence of the scattered light and constructing the time-dependent intensity correlation function

$$g^2(t) = \frac{\langle I(t)I(t+\tau)\rangle}{\langle I(t)\rangle^2} \qquad \text{Eq. 12}$$

Where *I(t)* and *I(t+τ)* are the intensities of the scattered light at times *t* and *t+τ* respectively, and the braces indicate averaging over *t*. From this correlation function translational diffusion coefficients can be determined from the decay rates of the relaxation modes [13]. The time-correlation function of the scattered field $g^1(t)$ for monodisperse particles has a mono-exponential shape and the corresponding decay rate, *Γ*, for these particles is

$$g^1(t) = \mathrm{e}^{-\Gamma \mathrm{t}},\ \Gamma = Dq^2 \qquad \text{Eq. 13}$$

D stands for the particle diffusion coefficient and q is the magnitude of the scattering wave vector defined as

$$q = \frac{4\pi n}{\lambda_0} \cdot \sin\left(\frac{\theta}{2}\right) \qquad \text{Eq. 14}$$

Where *n* is the refractive index of the solution, λ is the wavelength of light and θ the scattering angle. The electrical field correlation function $g^1(t)$ is related to the intensity correlation function $g^2(t)$ via the Siegert relation $g^1(t) = \sqrt{g^2(t) - 1}$.

For particles with low polydispersity the method of Cumulants can be used to determine the average size of particles [26]. The basis of the cumulant expansion lies in expanding the logarithm of g^1 in terms of the cumulants of the distribution. The correlation function can be analyzed by fitting a third-order polynomial to the intensity correlation function,

$$g^1(t) = A \cdot e^{-\overline{\Gamma}t + \frac{\Gamma^{(2)}}{2}\cdot t^2 - \frac{\Gamma^{(3)}}{6}\cdot t^3 + \cdots}$$

$$\ln\left(g^1(t)\right) = \mathrm{lnA} - \overline{\Gamma}\, t + \frac{\Gamma^{(2)}}{2} t^2 - \frac{\Gamma^{(3)}}{6} t^3 + \cdots \qquad \text{Eq. 15}$$

From the expansion, $\bar{\Gamma}$, is the first order cumulant corresponding to the first moment of the distribution and the hydrodynamic radius, R_H, can be determined by using the Stokes-Einstein equation (describes the diffusion of a spherical single particle)

$$R_H = \frac{k_B T}{6 \pi \overline{\Gamma}} q^2 \qquad \text{Eq. 16}$$

Another route is to use CONTIN, which is a DLS size-analysis software, from where one can get a qualitative analysis of the size distribution [12].

When particles are much smaller compared to the wavelength of the light used in the experiments, $r << \lambda$, the so-called collective diffusion coefficient or gradient diffusion coefficient, D_{coll}, is probed in dynamic light scattering. The diffusion coefficient corresponding to infinite dilute conditions, D_0 can be determined by plotting D_{coll} as a function of concentration, and by extrapolation, the intercept will yield D_0. This is the dilute-limiting diffusion coefficient which is correct to use in the Stokes-Einstein equation for determination of the hydrodynamic radius, R_H of the particles

$$R_H = \frac{k_B T}{6\pi\eta D_0} \qquad \text{Eq. 17}$$

Here η is the viscosity of the solvent. The hydrodynamic radius originates from the dynamics of a particle undergoing Brownian motion in a medium and the movements give rise to a frictional drag force [12].

$$\underline{F} = f\underline{v} \qquad \text{Eq. 18}$$

f is the frictional coefficient and $\underline{v}$ is the velocity. The frictional drag coefficient for a spherical particle was first given by Stokes

$$f = 6\pi\eta R_H \qquad \text{Eq. 19}$$

The relation between the kinetic energy of diffusion and frictional coefficient is

$$Df = k_B T \qquad \text{Eq. 20}$$

The Stokes-Einstein equation is obtained by introducing equation 19 into equation 20 [14].

$$D_0 = \frac{k_B T}{6\pi\eta R_H} \qquad \text{Eq. 21}$$

Small-Angle X-ray Scattering

In a Small-angle X-ray scattering (SAXS) experiment a collimated incoming beam of X-rays is directed onto a sample containing a solution of colloidal particles or macromolecules. The scattered light is detected as a function of scattering angle, which is proportional to q, defined as the difference between the incident vector (k_i) and the scattering vector (k_s) $q = k_s - k_i$ as shown in Figure 3 .

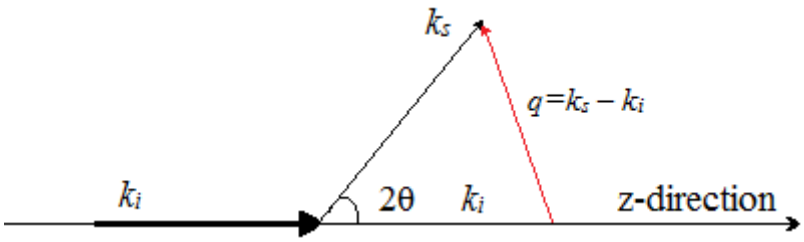

Figure 3. Definition of the scattering vector q as the difference between incident vector k_i and scattering vector k_s.

This is referred to as Rayleigh or Thomson scattering, which implies elastic scattering with little or no loss in energy when strongly bound electrons, when irradiated, start to oscillate at the same frequency as the incoming radiation. The distribution of the scattered X-rays is recorded in the plane of detection resulting in a 2D scattering pattern. Information about the structure and interactions of colloidal particles can be determined from analysis of the scattering pattern. The energy of the X-ray photons is much higher than the energy of visible light photons and the X-rays have a wavelength shorter than 0.3 nm which reflects the accessible length scales in SAXS.

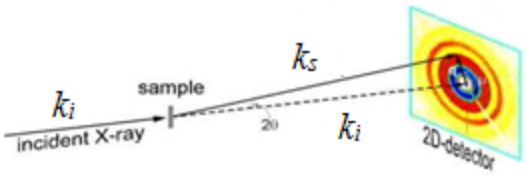

Figure 4. A schematic representation of X-ray scattering [16].

For isotropic scattering, a one-dimensional pattern is obtained by plotting the intensity as a function of the magnitude of the scattering vector q which for SAXS is defined as

$$q = \frac{4\pi}{\lambda} \cdot \sin\left(\frac{\theta}{2}\right)$$ Eq. 22

The scattered intensity of particles is related to the form factor *P(q)* and the structure factor *S(q)* by

$$I_s(q) = \frac{N}{V} P(q) S(q)$$ Eq. 23

where the form factor, *P(q)*, contains information about the shape and size of particles and the structure factor, *S(q)*, about particle interactions.

Materials and methods

Buffer 5 mM and 10 mM

Here I describe the steps and materials used in the preparation of the standard buffer 5 mM sodium acetate (NaOAc). This buffer is used for dissolving LF (bovine, ≥87 % Sigma).
Firstly, stock solutions of all components used in the standard buffer were prepared including sodium acetate trihydrate (NaOAc, <99 % Fluka), sodium azide (NaN_3, >99 %, Merck), sodium chloride (NaCl, 99.9 %, Sigma) and hydrogen chloride (37 %, Merck).

The mass needed (0.40824 g) to prepare 100 mL stock solution with a concentration of 30.0 mM NaOAc (M_w = 136.08 g/mol), was weighted and mixed with Millipore water in a volumetric flask and filtrated (0.45 µm, Minisart, Sartorius). The solution was transferred to a 100 mL glass bottle with a plastic cap and stored in the refrigerator prior to use. The stock solutions of sodium azide (NaN_3) and hydrogen chloride (HCl) were prepared in the same way and stored in the refrigerator, prior to use. The masses used in preparation of the stock solutions are given in Table 1, Appendix A.

As our standard buffer NaOAc was chosen at a pH 5.5 and ionic strength 5 mM, since it is far away from the isoelectric point, monovalent and LF is expected to be stable and monomeric [5]. The concentrations of NaOAc in the buffer solution were set to 3 mM, needed to ensure sufficient buffering capacity, also, the concentration of NaN_3 was chosen to 1 mM to prevent any bacterial growth. The amounts of all components used for preparing 500 mL of pH 5.5 5 mM NaOAc buffer are summarized in Table 1, Appendix A.

To prepare the final buffer, the required volumes of sodium acetate and sodium azide, taken from their respective stock solutions were mixed with Millipore water (425 mL) in an 500 mL E-flask. The pH was adjusted with addition of hydrogen chloride (see Table 2, Figure 16, Appendix A). The final concentration of added hydrogen chloride was 0.584 mM. The overall ionic strength in the buffer solution after addition of hydrogen chloride was 4.584 mM. In order to determine the volume of concentrated sodium chloride needed to reach the desired 5 mM ionic strength the following calculations were made.

$$C_{NaCl} = I_{total} - \left(I_{NaOAc} + I_{NaN_3} + I_{HCl}\right)$$
$$C_{NaCl} = 5\ mM - (3\ mM + 1\ mM + 0.584\ mM) = 0.416\ mM$$
$$0.416\ mM \cdot 500\ mL = 100{,}0\ mM \cdot V_{NaCl}$$

$$V_{NaCl} = \frac{0.416\ mM \cdot 500\ mL}{100.0\ mM} = 2.08\ mL$$

The resulting solution was transferred to a volumetric glass flask (500 mL) and Millipore water added until the total volume was 500 mL. The buffer solution was finally filtrated through a stack of two syringe filters (0.45 µm, Minisart, Sartorius) and transferred into two 250 mL glass flasks with glass stopper and stored in the refrigerator prior to use. Approximately 15 mL of buffer was used in the final pH determination, which gave a pH readingof 5.50.

The buffer with ionic strength of 10 mM and pH 5.5 for a volume of 100 mL was prepared in the same way as the 5 mM buffer. The amount of all components is found in Table 3, Appendix A. Finally, 15 mL of the buffer solution was taken for pH check, which gave pH of 5.50. The adjustment of the pH with hydrogen chloride is shown in Table 4 and Figure 17, Appendix A. All pH measurements were done with a PHM 210 Standard pH meter, Radiometer Copenhagen.

Preparation of concentrated lactoferrin stock solution

Lactoferrin (holo LF) powder (0.048 g, pink, fluffy flakes) was dissolved in 45 mL NaOAc buffer (5 mM at pH 5.5) in a Millipore pre-rinsed glass bottle (50 mL with a plastic cap). The concentration of the protein should be low in order to have en efficient dissolution of aggregates. The bottle was covered with parafilm and left in room temperature for 48 hours. The protein solution (slightly pink colour) was first filtrated with centrifugal filter (Amicon Ultra, 100 KDa, Merck Millipore) to remove agglomerates, which were found to be about 50 % of the dissolved powder consistently. In a second step the filtrate was transferred to a second centrifugal filter with a MWCO small enough to sustain the protein (Amicon Ultra10 KDa, Merck Millipore) and used both to washing away any existing ions or other unknown substances and buffer exchange. During the exchange procedure the protein solution is rinsed with buffer until the pH in the filtrate reaches a stable, unchanged value. The proteins are finally concentrated simply by not adding more buffer. The final solution of concentrated solution was transferred from the centrifugal filter to a Millipore prerinsed glass vial (2 mL). The centrifuge used for preparation of the protein solutions was a Sigma 4K 15 (details are shown in Table 5, Appendix B).

Concentration determination of lactoferrin

A UV-vis spectrophotometer (Varian, Cary WinUV) was used for absorbance measurements and determination of concentration. To ensure correct concentration determination in the spectrophotometer, DLS measurements were performed first to ensure monodisperse samples. Baselines were attained by absorbance measurements of the buffer solution between wavelengths ranging from 200 to 340 nm. The cuvette was washed with Millipore water in between measurements and dried with clean, compressed air. The optimal concentration of LF is around 1 mg/mL for concentration determination. The approximate volume of concentrated LF needed in order to obtain 1 mg/mL was calculated and transferred to the cuvette and the mass was recorded. Then the calculated amount of buffer was added and the total mass recorded. UV-vis measurements were performed again between 200-340 nm, and the concentration was determined using Beer Lambert law (equation 4).

Small-Angle Scattering Measurements

Dynamic and static light scattering measurements were performed at several concentrations in order to determine B_2 and D_{coll}. Dilution series with concentrations ranging between 5 and 50 mg/mL were prepared in glass vials (2 mL). Then the resulting solutions were transferred into NMR tubes (3 mm).

Before the DLS and SLS measurements were performed, the NMR tubes were carefully placed, to avoid scratches, in plastic centrifugal tubes and centrifuged for 10-40 minutes at 4000 rpm (corresponding to 3417 centrifugal force, CF) to spin down any dust to the bottom of the NMR tube in order to avoid disturbances during the light scattering measurements. The measurements were performed on a goniometer ALV DLS/SLS/ CGS8F (ALV GMBH, Langen, Germany).
The ALV goniometer is equipped with a Helium-Neon gas laser with a wavelength of 632.8 nm and output of 22 mW. The temperature is controlled to ± 0.1 ℃ by a water heating circulator. The temperature dependence measurements were done at 10, 25 and 37 °C. Angular scans were performed at six angles ranging from 50° to 140°.

Prior to any measurement, a short (30 s) DLS measurement was performed to ensure that the protein remained stable in its monomeric form. When the auto correlation function and distribution obtained from the CONTIN analysis showed good results, SLS measurements were performed at six angles ranging from 50° to 140° to a total of 48 measurements, each

with 30 s duration. The DLS measurements were performed at a fixed angle of 90° and measurement duration of 300 seconds per sample.

In the calculations, the refractive index value for pure water (1.332) was used for the solvent and a standard protein value for the value of the refractive index increment $1.9 \cdot 10^{-4}$ dn/dc [ml/mg] [25].

Preliminary SAXS measurements were done at the concentrations of 2, 23, and 33 mg/mL all in 5 mM, pH 5.5 buffer as well as for LF solution at concentrations 2 and 23 mg/mL in 10 mM, pH 5.5 buffer.

Results and discussion

During the washing step the pH of the filtrates from the centrifugal filter was monitored and the result is present in Figure 5. Data obtained from pH measurements is presented in the Table 6, Appendix B.

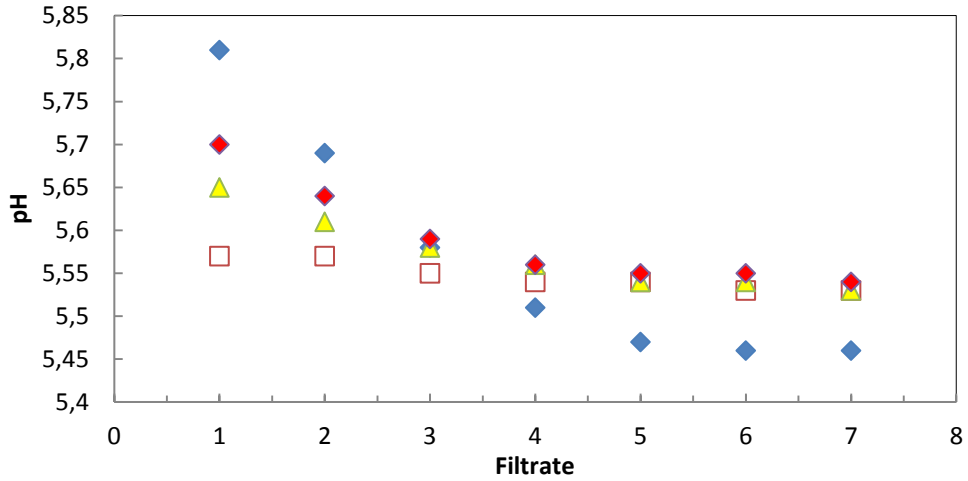

Figure 5. pH measurements of filtrates taken from different preparations of lactoferrin solutions (blue corresponds to the measurements using a different pH meter). Red filled squares correspond to preparation of LF in 10 mM buffer.

In order to determine the concentration of lactoferrin, the extinction coefficient was determined from absorbance measurements on a series of dilutions of known concentrations. The absorbance at 280 nm was plotted as a function of concentration is shown in Figure 7 which yielded a straight line.

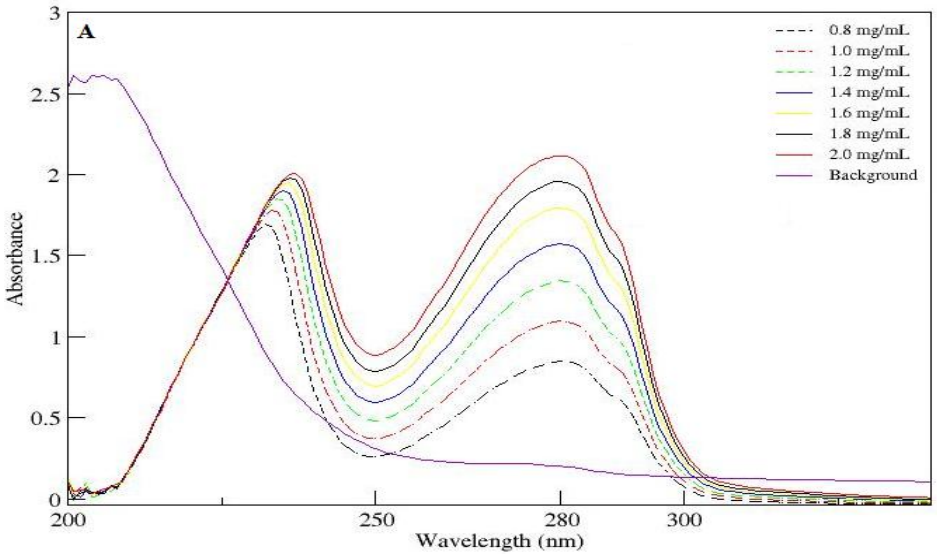

Figure 6. The absorbance spectrum for lactoferrin in NaOAc buffer at various concentrations (as shown in the figure legend).

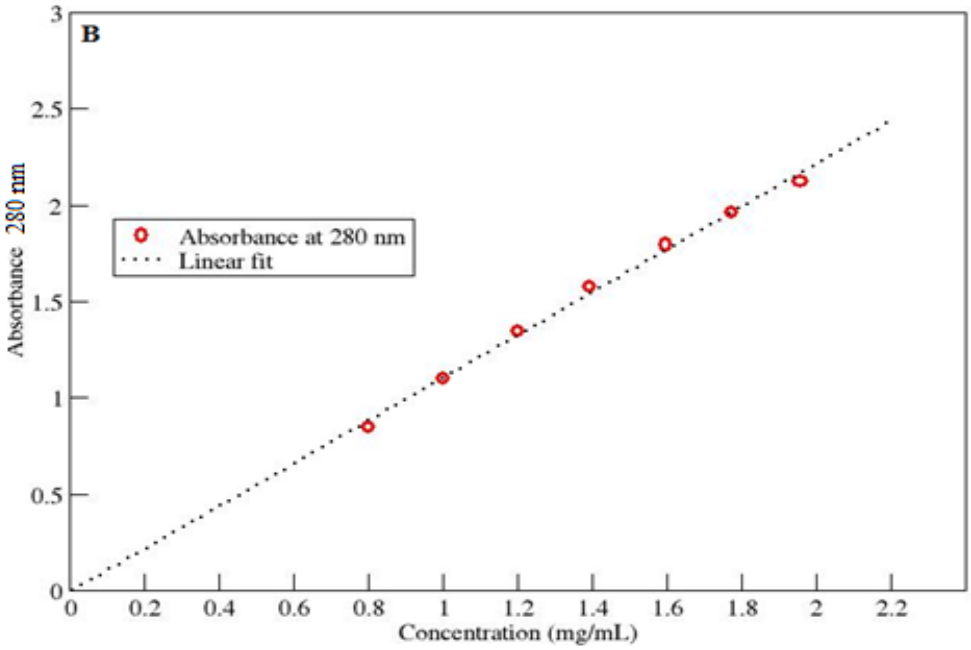

Figure 7. Determination of the extinction coefficient, ε, determined by plotting absorbance value at 280 nm as a function of concentration.

The maximum absorbance at series of dilutions is shown in Figure 6, which is then plotted as a function of concentration in Figure 7. The extinction coefficient is determined from the slope to be ε = 1.11026.

In the determination of concentrations, the mass of initial lactoferrin solution, the buffer and the total mass during dilution were noted on the balance in order to determine the dilution factor (by mass). Real concentrations were obtained by multiplying the concentration in the cuvette with the dilution factor (Eq. 24). Concentrated lactoferrin has intense red-brown colour, which comes from bound iron. In order to verify that the presence of the ions does not interfere with the DLS and SLS measurements, a UV-VIS spectrum was measured covering the wavelength used at SLS and DLS measurements, which is 632.8 nm. The result is shown in Figure 8 where it is only the typical peak at 280 nm arising from lactoferrin and no additional absorption peak at 632 nm, which means that the iron ions in the protein does not interfere with the light scattering measurements.

$$D = \frac{1}{m_{LF}/m_{tot}}$$

$$Concentration\ of\ LF = \frac{A}{\varepsilon \cdot l} \cdot D \qquad \text{Eq. 24}$$

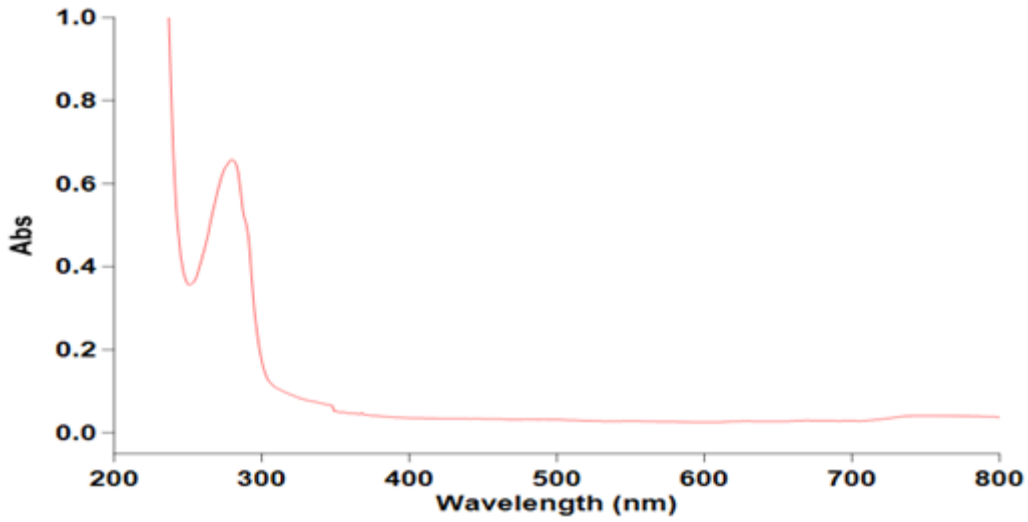

Figure 8. A broader ranged UV-VIS absorbance spectrum (800-200 nm) collected for a diluted LF sample.

In order to determine the second virial coefficient, B_2 and the collective diffusion coefficient, D_{coll}, both static and dynamic light scattering measurements were performed as a function of concentrations.

The highest concentration used here was 62.111 mg/mL. Six samples with different concentrations were prepared see Table 7 in Appendix D and reduced Zimm plots obtained for these LF samples both in 5 mM and 10 mM NaOAc buffer at pH 5.5 are shown in Figure 9. As expected both ionic strengths have large positive slopes and give highly positive B_2 values telling of overall strong repulsive interactions between the LF molecules. Data for LF in 5 mM buffer from two separate preparations gives close to identical slopes showing that the protein and sample preparation is robust and produce quantitatively reproducible results. When ionic strength of the buffer was increased from 5 to 10 mM, at a constant pH, the slope and thus B_2 decreased substantially. This means that the interactions between the proteins are much less repulsive at a slightly higher ionic strength. The molecular weights of lactoferrin obtained from the intercept are 79.4 kg/mol, 77.7 kg/mol and 75.9 kg/mol respectively, are in good agreement with the literature values [1-4].

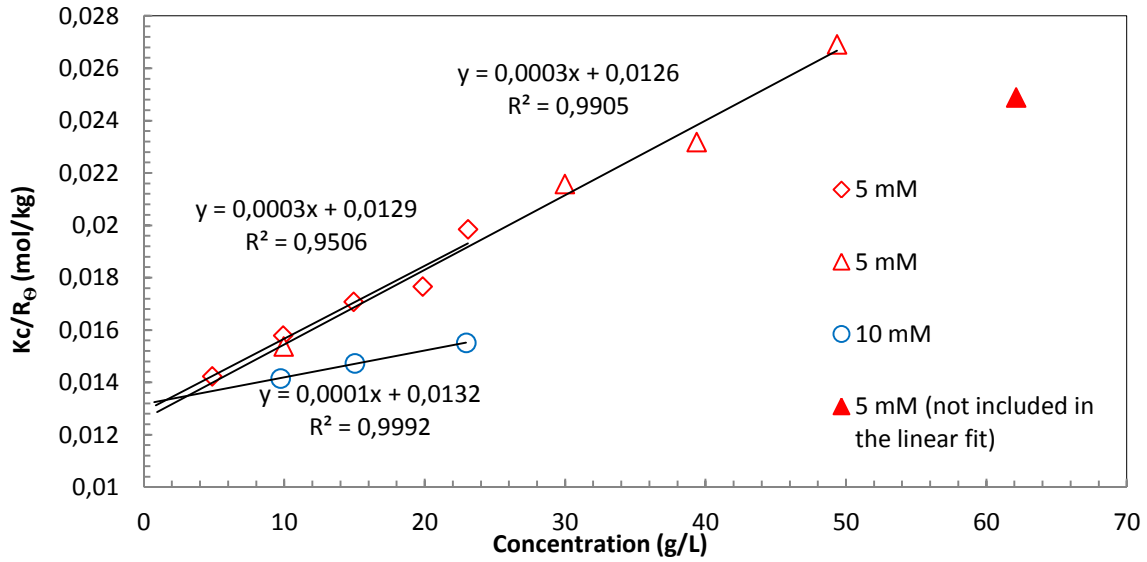

Figure 9. Reduced Zimm plot for lactoferrin dissolved in 5 mM buffer (red triangles and squares) and 10 mM buffer (blue circles).

In Figure 9, higher concentrations (≥ 50 mg/mL) a deviation from the linear dependence is observed. Here, the effect from higher order terms in the virial expansion becomes more dominant at higher concentrations, for this reason, these concentrations were not included in the linear regression.

Normalized B_2 values (B_2/B_2^{HS}) as a function of ionic strength are shown in Figure 10. The second virial coefficient decreases strongly from 9 to 3 when ionic strength is increased from 5 to 10 mM. This drop in B_2 is expected and is due to screening by a decrease in the electrostatic repulsions on addition of electrolyte.

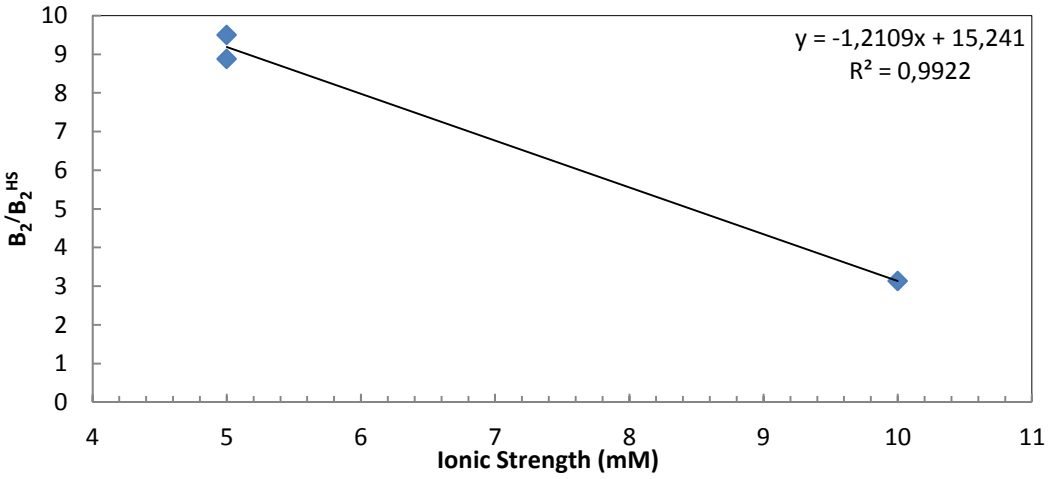

Figure 10. Normalized second virial coefficients as a function of ionic strength.

Light scattering measurements were performed at three different temperatures (10, 22 and 37 °C) in order to investigate how the interactions, captured by B_2, vary with temperature. This is shown in Figure 11 where normalized second virial coefficients are plotted as a function of temperature see Table 11 in Appendix E. The values were normalized with the mean value of B_2^{HS} determined from three consecutive measurements of the collective diffusion coefficient extrapolated to zero concentration (Table 11 in Appendix E).

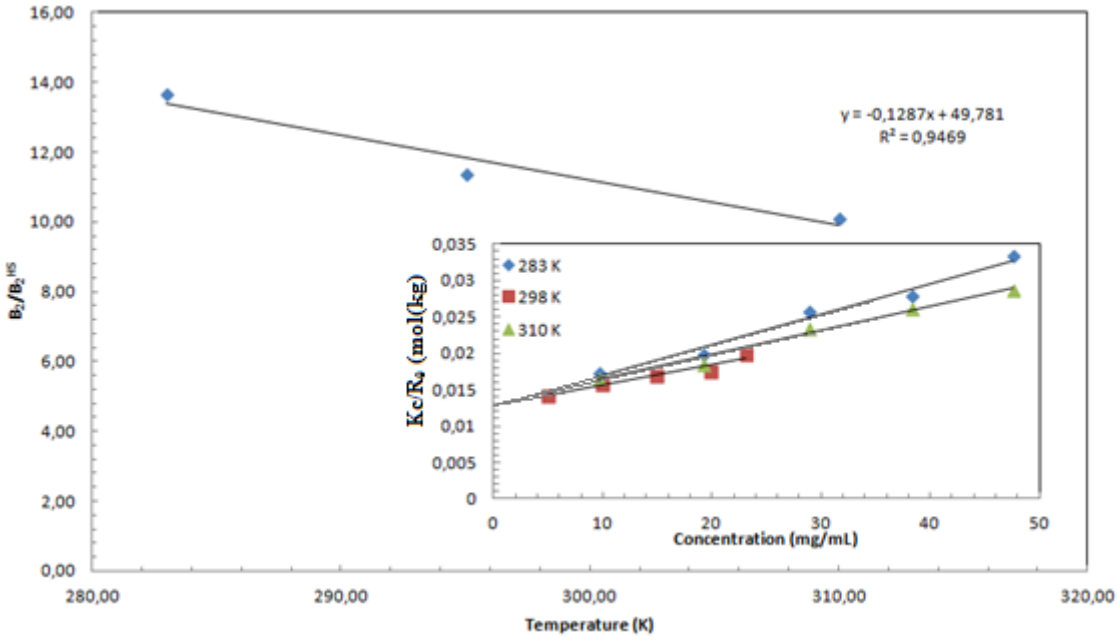

Figure 11. The normalized second virial coefficient (B_2/B_2^{HS}) as a function of temperature. The inset shows the corresponding reduced Zimm plots from which B_2 was determined.

We observe a decrease in the second virial coefficient from 13.6 (at 10 °C) to 10.1 (at 37 °C). This means that with increasing temperature the proteins becomes more attractive or less repulsive. The reason for this slight decrease in B_2 is presumably due to a second order effect in the van der Waals forces, from fluctuations of dipoles, which becomes notable due to the very low salt concentration. When the temperature is increased the amplitude of the fluctuations increases resulting in stronger dipole-dipole interactions and van der Waals forces. If we would have higher salt concentration, then hydrophobic interactions would be more prominent, and we would expect to see the opposite result with B_2 increasing at higher temperatures.

In order to determine the diffusion coefficients corresponding to the Stokes-Einstein single sphere, the D_{coll} obtained from DLS, is plotted as a function of concentration, as shown in

Figure 12. The intercept with the y-axis corresponds to this dilute-limiting diffusion coefficient, D_0.

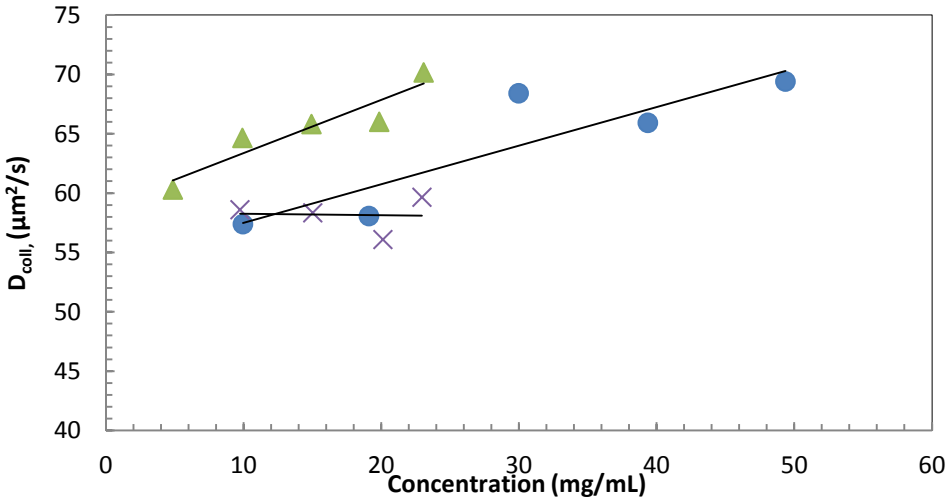

Figure 12. The collective diffusion coefficients plotted as a function of LF concentration. The intercept gives the D_0. The blue circles and green triangles correspond to 5 mM buffer and red squares correspond to 10 mM buffer (both at 25.0 °C).

The hydrodynamic radius, $R_{H,}$ was determined using the Stokes-Einstein equation (18) at zero concentration, in Figure 12. The second virial coefficient for hard spheres (equation 11, Table 12, Appendix E) was calculated using this hydrodynamic radius. The result is presented in Table 12. Three measurements gave approximately the same hydrodynamic radius of 4.2 nm, and in a good agreement with the literature value [5].

Light scattering measurements on LF dilution series (10-50 mg/mL) performed at five different angles (50° – 145°) are shown in Figure 13. As expected, there is no change in the slope with varying scattering angle meaning that there is no angular dependency.

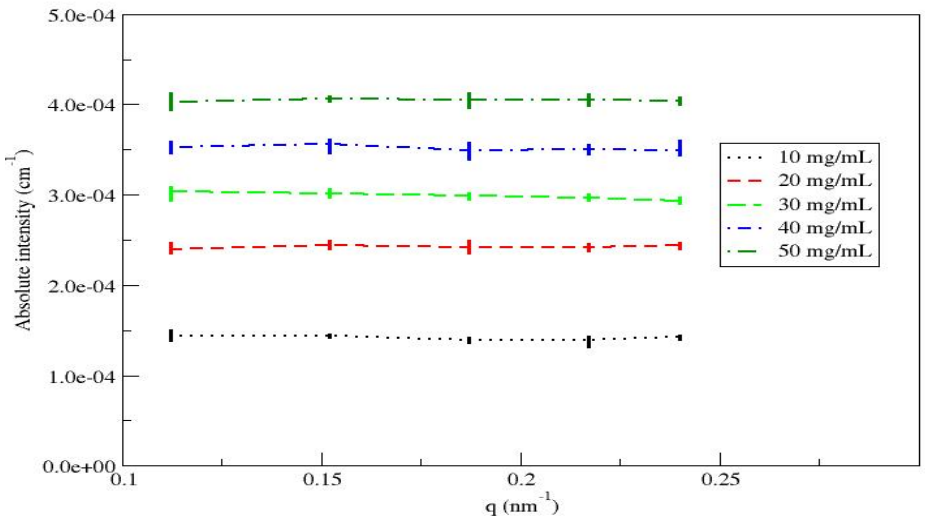

Figure 13. Angular dependency measurements of lactoferrin in NaOAc buffer, pH 5.5 at 5 mM ionic strength.

The stability of the proteins in solution was investigated for lactoferrin in order to see if any aggregates formed over time. In Figure 14 the distribution of hydrodynamic radius remains narrow and unchanged with time, where time interval between each measurement was 7-10 days.

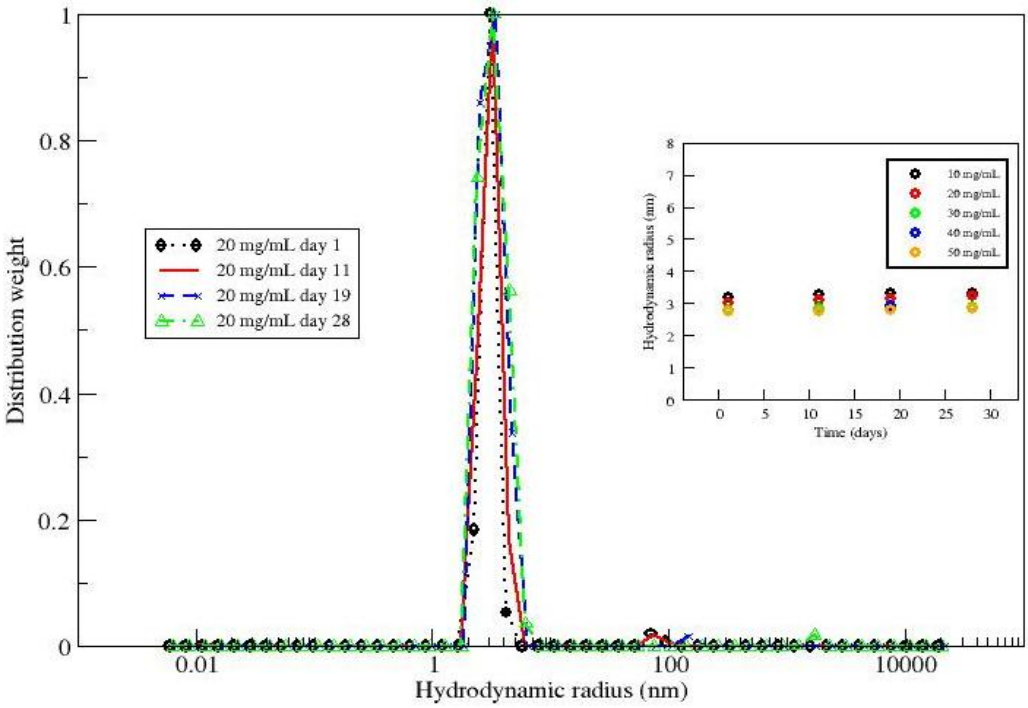

Figure 14. The time stability is here shown as the time evolution of the hydrodynamic radius. The distribution of radius is obtained from the ALV software, using the nonlinear fit method (the CONTIN routine).

SAXS measurement on lactoferrin (33 mg/mL) in 5 mM buffer is presented below and the forces acting between molecules are envisaged by a decrease in the low *q* scattering, which is expected for repulsive interactions.

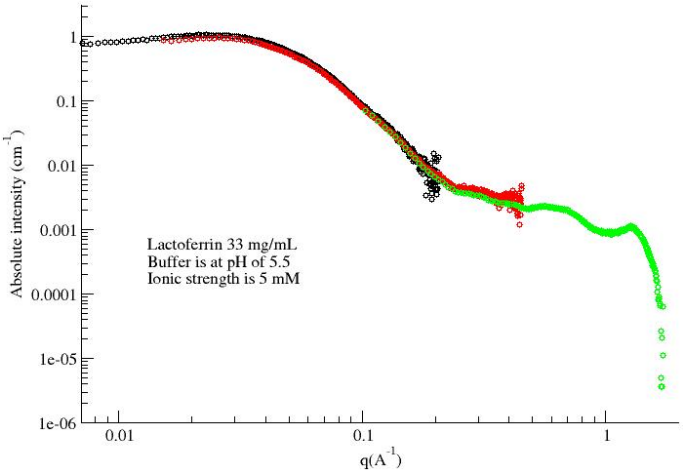

Figure 15. Intensity as a function of q(Å^{-1}) at a concentration of 33 mg/mL LF.

Conclusions and future work

The correlation functions obtained from the light scattering measurements showed single exponentials, with a rapid decay indicating the absence of particles with sizes bigger than LF (~4 nm). The Contin regular fitting showed one narrow peak corresponding to the same size between 3-4 nm. At pH 5.5 and ionic strength 5 mM and 10 mM LF stayed in monomeric form. From the time dependence measurements on LF in 5 mM buffer solution it was shown that there is no aggregate formation up to 25 days (Figure 14). As it was expected the second virial coefficient decreased when the ionic strength of buffer was increased. Temperature dependence measurement made at 10°C, 25°C and 37°C, showed that B_2 weakly decreases with increasing temperature (Figure 11), which most likely originates from second order effects in the electrostatics due to increased dipole fluctuations. Preliminary SAXS measurements revealed that at 5 mM and pH 5.5 the interactions between LF molecules are repulsive.

For future aspects the second virial coefficient should be determined at higher pH approaching the LF isoelectric point. By increasing pH the net charge of LF will decrease, causing changes in electrostatic patches. B_2 should also be obtained for higher salt concentrations. According to computer simulations, the second virial coefficient will decrease with increased ionic strength until it riches a minimum and further addition of salt will act to increase B_2, due to the presence of attractive patch on the surface of the protein. This is currently under investigation.

Acknowledgements

I would like to thank my supervisor Malin Zackrisson Oskolkova for her engagement and support during my bachelor thesis, especially with correcting it. I would also like to thank my co-supervisor Weimin Li for his helpful advises and his time which he spent helping me with measurements. In addition, I thank Solmaz Bayati for her time she put on explaining me the basic concepts of ALV. Furthermore I wish to thank all those who participated in my presentation and the examiner Anna Stradner in particular.

References

1. L. Adlerova, A. Bartoskova, M. Faldyna, *Vet. Med.*, **53**, 457 (2008)
2. S. A. González-Chávez, S. Arévalo-Gallegos, Q. Ranscón-Cruz, *Int. J. of Antimicrob. Agents*, **33**, 301.e1-301.e8 (2009)
3. B. A. Persson, M. Lund, J. Forsman, D. E. W. Chatterton, T. Åkesson, *Biophys. Chem.*, **151**, 187 (2010)
4. van der Strate BWA, Belijaars L, Molema G, Harmsen MC, Meijer DK, *Antiviral Res*. **52**, 225, (2001)
5. I. Mela, E. Aumaitre, A. M. Williamson, G. E. Yakubov, *Colloid Surface B*, **78**, 53, (2010)
6. A. Sreedhara, R. Flengsrud, T. Langsrud, P. Kaul, V. Prakash, G. E. Vegarud, *Biometals*, **23**, 1159, (2010)
7. Y. Liang, W, R. Bowen, *J. Coll. Int. Sci.*, **284**, 157, (2005)
8. S.A Moore, B. F. Anderson, C. R. Groom, M. Haridas, E. N. Baker, *J. Mol. Biol*. **274**, 222, (1997)
9. Peter Atkins and Julio de Paula, Physical Chemistry, 9th ed, (2009).
10. http://www.microspectra.com/component/content/article/35-technical-support/185-protein-absorbance
11. J. K. G. Dhont, *An Introduction to dynamics of colloids*, Elsevier, 1996.
12. R. Piazza, M. Pierno, S. Iacopini, P. Mangione, G. Esposito, V. Bellotti, *Eur. Biophys. J.* **35**, 439, (2006)
13. I. W. Hamley, *Introduction to soft matter, revised edition, 11-12, (2007).*
14. H. Schnablegger, Y. Singh, The SAXS Guide, (2011).
15. http://what-when-how.com/wp-content/uploads/2011/05/tmp127118_thumb.jpg
16. http://sni-portal.uni-kiel.de/kekm-bilder/Instrumentenzugang/saxs.jpg
17. I. W. Hamley, *Introduction to soft matter, revised edition, (2007).*
18. http://www.substech.com/dokuwiki/lib/exe/fetch.php?w=&h=&cache=cache&media=electric_double_layer.png
19. Manual to ALV Goniometer, The ALV-NonLinear Data Analysis, Cumulant data analysis.
20. R. Piazza, *Current Opinion in Colloid and Interface Science* **8**, 515, (2004)
21. A. C. Dumetz, A. M. Chockla, E. W. Kaler, A. M. Lenhoff, *Biochem. et Biophys. Acta* **1784**, 600, (2008)
22. M. Boström, F. W. Tavares, S. Finet, F. Skouri-Panet, A. Tardieu, B. W. Ninham, *Biophys. Chem.*, **117**, 217, (2005)
23. J. G. Kirkwood, J. B. Shumaker, **38**, (1952)
24. F. Sciortino, *Eur. Phys. J. B*, **64**, 505, (2008)
25. T. Gibaud, F. Cardinaux, J. Bergenholtz, A. Stradner, P. Schurtenberger.
26. D. E. Koppel, *J. Chem. Phys.*, **57**, 11, (1972)

Appendix

A. Buffer preparation

Table 1. The amount of chemicals used for preparation of 500 ml buffer solution with ionic strength 5 mM and pH 5.5.

Chemical	**Concentration of stock solution (mM)**	**Buffer concentration (mM)**	**Volume of stock solution (mL)**
NaOAc	30,019	3,0	49,968
NaN_3	101,677	1,0	4,918
HCl	104,188	0,584	2,8
NaCl	100,0	0,416	2,08

Table 2. The adjustment of pH to a final value of 5.5 in NaOAc buffer upon addition of HCl (104.188 mM). A volume of 200 µL was added repeatedly to a final volume of 2800 µL. Lastly, the ionic strength was adjusted to 5 mM.

Injection volume of HCl (µL)	**Total volume of HCl (µL)**	**pH with stirring**	**pH without stirring**
0	0	6,96	6,98
200	200	6,53	6,55
200	400	6,31	6,33
200	600	6,17	6,19
200	800	6,05	6,07
200	1000	5,96	5,98
200	1200	5,88	5,90
200	1400	5,81	5,82
200	1600	5,75	5,77
200	1800	5,69	5,71
200	2000	5,64	5,68
200	2200	5,59	5,61
200	2400	5,55	5,57
200	2600	5,51	5,53
200	2800	5,47	5,49

Table 3. The amount of chemicals used for preparation of 100 mL buffer with ionic strength of 10 mM and pH 5.5.

Chemical	Concentration of stock solution (mM)	Buffer concentration (mM)	Volume of stock solution (mL)
NaOAc	30,019	3,0	9,994
NaN_3	101,677	1,0	0,9835
HCl	104,188	0,584	0,560
NaCl	100,0	5,416	5,416

Table 4. The adjustment of the pH in 10 mM buffer solution with hydrogen chloride (104.188 mM). Total volume of added HCl is 560 µL.

Injection volume of HCl (µL)	Total volume of HCl (µL)	pH with stirring	pH without stirring
0	0	7,02	7,05
100	100	6,25	6,28
100	200	5,96	5,99
100	300	5,78	5,80
100	400	5,64	5,67
100	500	5,53	5,56
20	520	5,51	5,53
20	540	5,49	5,51
20	560	5,47	5,49

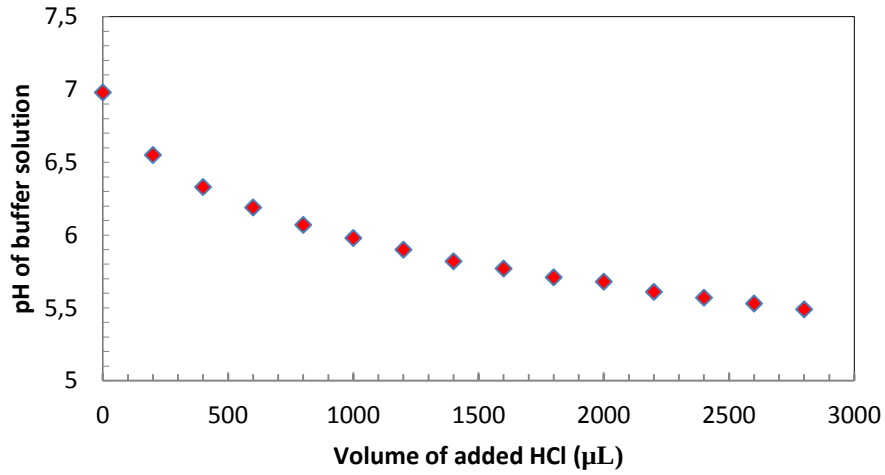

Figure 16. The pH adjustment of the 5 mM buffer solution.

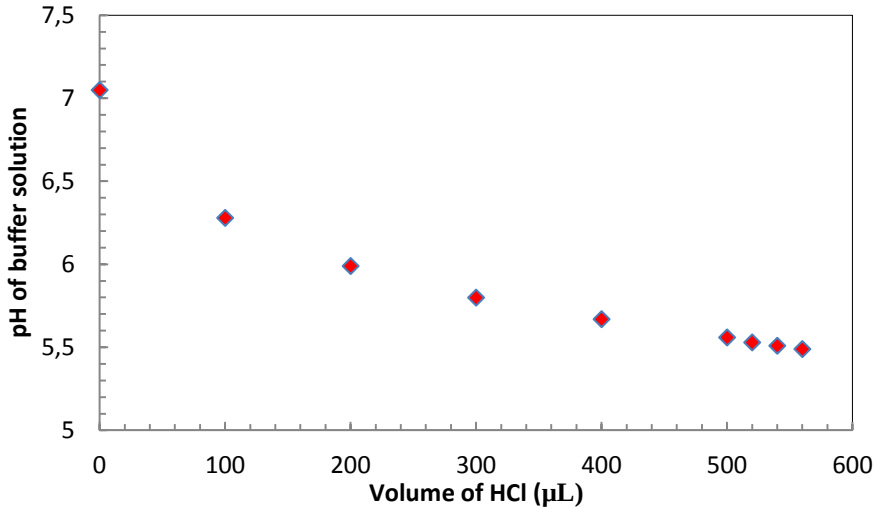

Figure 17. The pH adjustment of the 10 mM buffer.

B. Sample preparation

Table 5. Centrifuge mode for filtration and concentration of lactoferrin solutions.

Type	**Speed**	**Centrifugal force**	**Temperaute, (°C)**
Swing-out rotor for 6 buckets 11156/13127	4000 rpm	3417 rcf	22

Table 6. pH measurements of filtrates from 10 K Amicon Ultra centrifugal filters containing LF solutions.

Filtration	**pH Lactoferrin 2**	**pH Lactoferrin 3**	**pH lactoferrin 5 (5 mM)**	**pH Lactoferrin 5 (10 mM)**
1	5,81	5,57	5,65	5,70
2	5,69	5,57	5,61	5,64
3	5,58	5,55	5,58	5,59
4	5,51	5,54	5,56	5,56
5	5,47	5,54	5,54	5,55
6	5,46	5,53	5,54	5,55
7	5,46	5,53	5,53	5,54

C. Concentration determination

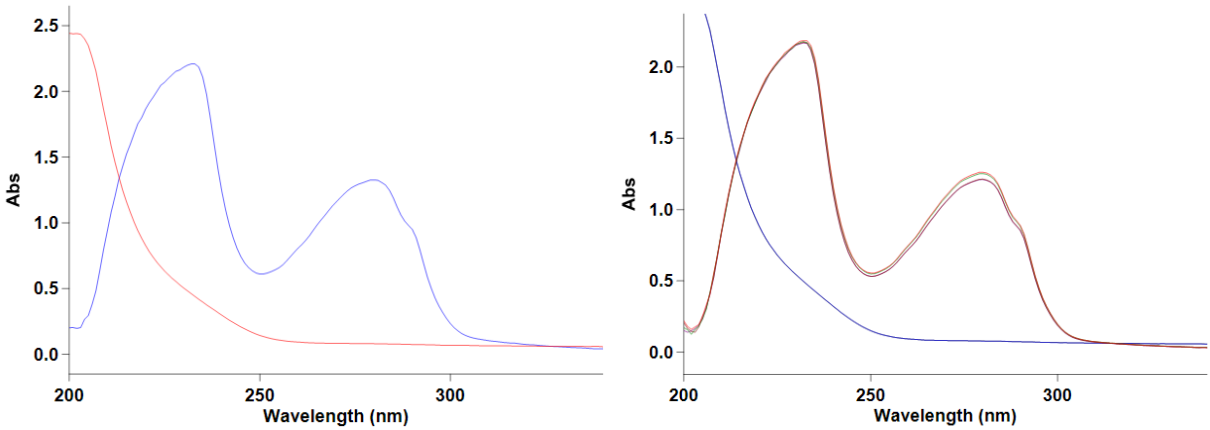

Figure 18. Absorption spectrum of lactoferrin solutions in 5 mM buffer.

D. Dilutions for light scattering measurements

Table 7. Dilution series of lactoferrin from the second preparation. The amount of concentrated sample was approximately 250 µl, which is less than needed the volume. Concentrations 40, 30 and 10 mg/ml were prepared from 62.50 and 20 mg/ml respectively by adding buffer directly to NMR tubes.

Series number	**LF concentration for B_2 C_1 (mg/ml)**	**Final volume V_1 (µl)**	**Volume C_2 (µl)**	**Volume buffer (µl)**
1	62,111	80	80	0
2	50	80	64,401	15,599
3	40	80	51,521	28,479
4	30	80	38,640	41,360
5	20	80	25,760	54,240
6	10	80	12,880	67,120
Total Volume (µl)			**273,202**	**206,798**
	Real concentration (mg/ml)	**Mass of C_2 (g)**	**Mass Buffer (g)**	**Total Mass (g)**
1	49,356	0,0623	0,0161	0,0784
2	39,969 (Diluted 62,111 mg/ml)	0,0926	0,0513	0,1439
3	29,973 (Diluted 49,356 mg/ml)	0,0623	0,0507	0,1291
4	19,099	0,0241	0,0543	0,0788
5	9,946 (Diluted 19,099)	0,0241	0,0717	0,1505

Table 8. Dilution series of lactoferrin from the third preparation. All dilutions were prepared directly in the NMR tubes.

Series number	**LF concentration for B_2 C_1 (mg/ml)**	**Final volume V_1 (µl)**	**Volume C_2 (µl)**	**Volume buffer (µl)**
1	54,702	80	80	0
2	50	80	73,123	6,877
3	40	80	58,449	21,501
4	30	80	43,874	36,126
5	20	80	29,249	50,751
6	10	80	14,625	65,375
Total Volume (µl)			**299,370**	**180,630**
	Real concentration (mg/ml)	**Mass of C_2 (g)**	**Mass Buffer (g)**	**Total Mass (g)**
1	47,540	0,0697	0,0105	0,0802
2	38,215	0,0554	0,0239	0,0793
3	28,790	0,0390	0,0351	0,0741
4	19,155	0,0291	0,0540	0,0831
5	9,544	0,0138	0,0653	0,0791

Table 9. Dilution series for lactoferrin from the fifth preparation in 5 mM buffer.

Series number	**LF concentration for B2 C_1 (mg/ml)**	**Final volume V_1 (µl)**	**Volume C_2 (µl)**	**Volume buffer (µl)**
1	23,076	80	80	0
2	20	80	69,336	10,664
3	15	80	52,002	27,998
4	10	80	34,668	45,332
5	5	80	17,334	62,666
Total Volume (µl)			**253,340**	**146,660**
	Real concentration (mg/ml)	**Mass of C_2 (g)**	**Mass Buffer (g)**	**Total Mass (g)**
1	23,076	0,0789	0	0,0789
2	19,876	0,0677	0,0110	0,0786
3	14,928	0,0502	0,0274	0,0776
4	9,910	0,0347	0,0461	0,0808
5	4,858	0,0168	0,0630	0,0798

Table 10. Dilution series for lactoferrin 5 in 10 mM buffer.

Series number	**LF concentration for B2 C_1 (mg/ml)**	**Final volume V_1 (µl)**	**Volume C_2 (µl)**	**Volume buffer (µl)**
1	22,951	80	80	0
2	20	80	69,714	10,286
3	15	80	52,285	27,715
4	10	80	34,857	45,143
5	5	80	17,428	62,572
Total Volume (µl)			**254,284**	**145,716**
	Real concentration (mg/ml)	**Mass of C_2 (g)**	**Mass Buffer (g)**	**Total Mass (g)**
1	22,951	0,0783	0	0,0783
2	20,115	0,0688	0,0102	0,0785
3	15,019	0,0498	0,0263	0,0761
4	9,731	0,0329	0,0448	0,0777
5	4,730	0,0163	0,0628	0,0791

E. Light Scattering

Values for the slope, the intercept, B_2, B_2^{HS}, normalized B_2^* (B_2/B^{HS}), molecular weight (M_W) are presented in table 11. B_2 of hard spheres was determined from dynamic light scattering by measuring the collective diffusion coefficient (D_{coll}). Value of B_2^{HS} presented in the table below is a mean value of three measurements.

Table 11. Data used for determination of second virial coefficient for lactoferrin at 5 mM and 10 mM buffer. Values of B_2 at 10°C, 25°C and 37°C are shown.

Lactoferrin preparation no.	**Slope**	**Intercept**	**M_W (kg/mol)**	**B_2 (m^3)**	**$B_{2\ Hard\ Sphere}$ (m^{-3})**	**B_2/B_2^{HS}**
2 (5 mM)	2,751E-4	1,260E-2	79,386	1,491E-24	1,571E-25	9,947
3 (5 mM)	3,614E-4	1,563E-2	63,965	1,784E-24	1,571E-25	11,354
5 (5 mM)	2,786E-4	1,288E-2	77,647	1,395E-24	1,571E-25	8,877
5 (10 mM)	1,027E-4	1,316E-2	75,963	4,921E-25	1,571E-25	3,133
Temperature dependence (5 mM buffer)						
3 (10°C)	4,208E-4	1,277E-2	78,303	2,142E-24	1,571E-25	13,636
5 (25°C)	2,786E-4	1,288E-2	77,647	1,395E-24	1,571E-25	8,877
3 (37°C)	3,337E-4	1,321E-2	75,716	1,588E-24	1,571E-25	10,110

Table 12. Values of infinite dilution diffusion coefficient, hydrodynamic radius and B_2 of hard spheres.

Lactoferrin preparation no	**Diffusion coefficient, D_0 ($\mu m^2/s$)**	**Hydrodynamic radius, (nm)**	**B_2^{HS}**
2 (5 mM)	54,240	4,220	1,574E-25
5 (5 mM)	58,895	4,161	1,509E-25
5 (10 mM)	57,503	4,269	1,629E-25